Since January 2020 Elsevier has created a COVID-19 resource centre with free information in English and Mandarin on the novel coronavirus COVID-19. The COVID-19 resource centre is hosted on Elsevier Connect, the company's public news and information website.

Journal of Structural Biology 214 (2022) 107879

Contents lists available at ScienceDirect

Journal of Structural Biology

journal homepage: www.elsevier.com/locate/yjsbi

Structural basis for SARS-CoV-2 nucleocapsid (N) protein recognition by 14-3-3 proteins

Andrea Eisenreichova, Evzen Boura *

Institute of Organic Chemistry and Biochemistry AS CR, v.v.i., Flemingovo nam. 2, 166 10 Prague 6, Czech Republic

ARTICLE INFO

Edited by 'Andreas H Engel'

ABSTRACT

14-3-3 proteins are important dimeric scaffolds that regulate the function of hundreds of proteins in a phosphorylation-dependent manner. The SARS-CoV-2 nucleocapsid (N) protein forms a complex with human 14-3-3 proteins upon phosphorylation, which has also been described for other coronaviruses. Here, we report a high-resolution crystal structure of 14-3-3 bound to an N phosphopeptide bearing the phosphoserine 197 in the middle. The structure revealed two copies of the N phosphopeptide bound, each in the central binding groove of each 14-3-3 monomer. A complex network of hydrogen bonds and water bridges between the peptide and 14-3-3 was observed explaining the high affinity of the N protein for 14-3-3 proteins.

14-3-3 proteins are a class of universal molecular scaffolds that are known to have more than 300 binding partners and are conserved from yeast to human (Eisenreichova et al., 2016). Humans have seven isoforms (β, ε, η, γ, τ, ζ, σ) that form homo- and heterodimers and recognize their binding partners almost exclusively in a phosphorylation-dependent manner (Obsilova et al., 2008; Sluchanko, 2020). Upon phosphorylation of the client protein, a complex between the client and the 14-3-3 protein is formed, and the function of the client protein is altered. Alterations include inhibition or activation of enzymatic activity (Alblova et al., 2017; Obsilova and Obsil, 2020), modified subcellular localization (often nuclear import is blocked) (Obsilova et al., 2005) or transformed accessibility of post-translational modification sites (Horvath et al., 2021). Further, a change in the stability of the client protein (Chalupska et al., 2017) or in the interaction with 14-3-3 putatively influences the ability of the client protein to form other protein:protein complexes (Rezabkova et al., 2010).

The SARS-CoV-2 nucleocapsid (N) protein consists of two RNA binding domains, termed NTD and CTD (N- and C-terminal domain) and three intrinsically disordered regions (IDR1-3), and it is heavily phosphorylated (Bai et al., 2021; Carlson et al., 2020; Gao et al., 2021; Rozycki and Boura, 2022; Tung and Limtung, 2020). Within the IDRs, several motifs resemble the two optimal 14-3-3 binding motifs: RSX(pS/pT)XP and RX(Y/F)X(pS/pT)XP. Indeed, it was described that the N forms a protein complex with 14-3-3 proteins upon its phosphorylation with a 2:2 stoichiometry (one N dimer binds one 14-3-3 dimer), and pS197 was identified as the key phosphorylated residue of the N protein (Tugaeva et al., 2021).

We aimed to understand the formation of the 14-3-3:N protein complex at the atomic level; therefore, we decided to solve the crystal structure of a phosphorylated N peptide (residues 194-SRNpSTPG-200) bound to 14-3-3. We expressed and purified the 14-3-3 (ζ isoform) as described before (Eisenreichova et al., 2016) (detailed in SI) and mixed it with the 194-SRNpSTPG-200 phosphopeptide in a 1:1 molar ratio. We screened for crystals using the sitting drop approach where 200 nl of the protein mixture was mixed with 200 nl of the well solution from JCSG I-IV commercial screens (QIAGEN). The initial crystals ruptured during cryo-protection, hence a second round of screening in the same way was performed using screens supplemented with glycerol (20% v/v). Eventually we obtained well diffracting crystals that belonged to the orthorhombic $P2_12_12_1$ spacegroup and diffracted to 1.9 Å resolution. The structure was solved by molecular replacement and refined to R_{work} = 18.38% and R_{free} = 20.34% and good geometry (SI Table 1) using the Phenix crystallographic package (Afonine et al., 2018; Liebschner et al., 2019) and deposited in the PDB under the accession code 7ZIT.

The electron density for the whole N peptide was clearly visible immediately after molecular replacement (Fig. 1A and B). Two copies of the peptide were found, each in the central binding groove of both 14-3-3 monomers that is formed by helices α3, α5, α7 and α9 (Fig. 1A). Close inspection of the N binding mode revealed a complex web of hydrogen bonds and water bridges (Fig. 1C and D) that explain the recently reported high affinity of this site for 14-3-3 proteins (Tugaeva et al., 2021). The phospho-head group of pS197(N) is directly recognized by residues

* Corresponding author.
E-mail address: boura@uochb.cas.cz (E. Boura).

https://doi.org/10.1016/j.jsb.2022.107879
Received 30 May 2022; Received in revised form 24 June 2022; Accepted 28 June 2022
Available online 30 June 2022

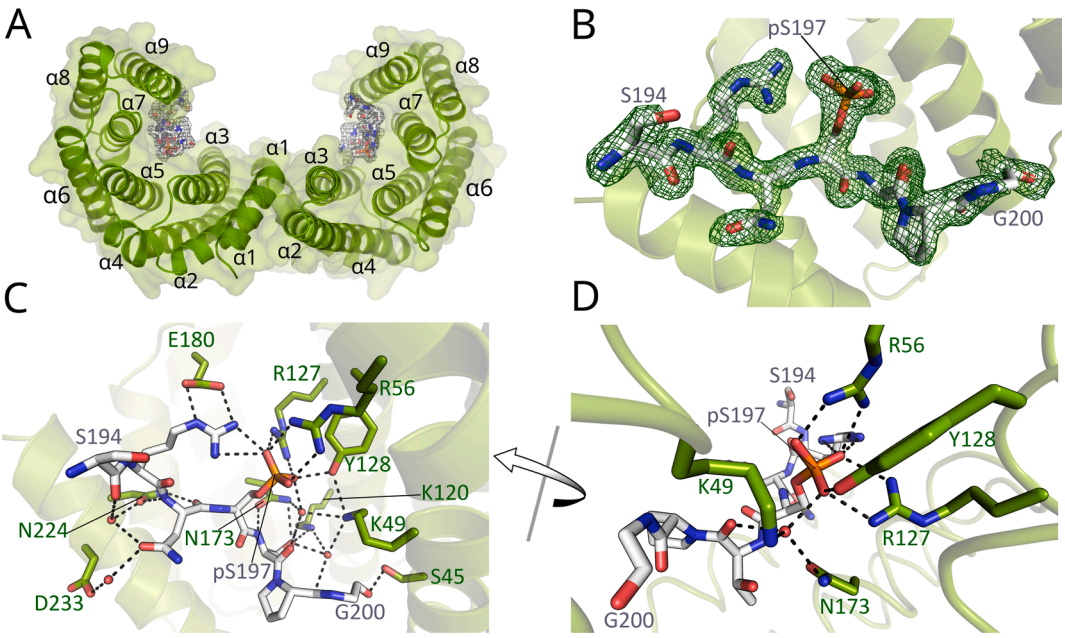

Fig. 1. The crystal structure of the SARS-CoV-2N protein-derived phosphopeptide bound to human 14-3-3ζ. (A) The overall fold. The 14-3-3 dimer can accommodate two N phosphopeptide molecules. 14-3-3 is coloured green and is depicted in both the cartoon and the semi-transparent surface representation. (B) Electron density of N-protein phosphopeptide (white sticks) is shown in the Fo-Fc omit map contoured at 3σ and coloured in green. (C) Detailed view of the phosphorylated N peptide in the 14-3-3ζ binding groove. The N peptide is shown in the white in stick representation. 14-3-3 is coloured green and the peptide-interacting 14-3-3 residues are represented as sticks. Polar interactions are depicted as black dotted lines. Water molecules engaged in the interaction are shown as red spheres. (D) Detailed view of the N-peptide phosphoserine (pS197) and its polar interactions (black dotted lines). (For interpretation of the references to colour in this figure legend, the reader is referred to the web version of this article.)

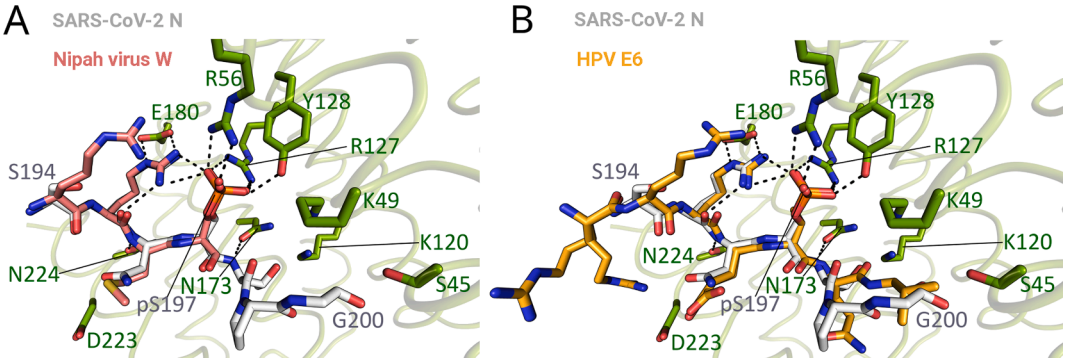

Fig. 2. Superposition of 14-3-3 bound viral peptides. (A) Structural alignment of the SARS-CoV-2N-protein phosphopeptide (white sticks) with phosphopeptide from Nipah virus W protein (PDB ID:6W0L, pink sticks). Polar interactions common to both peptides are depicted as black dotted lines. (B) SARS-CoV-2N protein-phosphopeptide (white sticks) superimposed to peptide derived from the PBM domain of the E6 protein of HPV type 18 (PDB ID 6ZFD, orange sticks). (For interpretation of the references to colour in this figure legend, the reader is referred to the web version of this article.)

R56, R127 and Y128. Interestingly, the observed conformation of the N phosphoprotein is stabilized by an intramolecular hydrogen bond between the phospho-head group and adjacent sidechain or R195(N). This arginine residue is also held in place by two hydrogen bonds with E180. Further, the sidechains of N196(N) and T198(N) are directly recognized by the 14-3-3 protein: N196(N) forms a water bridge with D233, and T198(N) forms hydrogen bonds with K49 and N173. In addition, the backbone of the N phosphopeptide forms numerous hydrogen bonds with the 14-3-3 protein (Fig. 1C).

14-3-3 was also reported to interact with many viral proteins (Boon and Banks, 2013; Nathan and Lal, 2020). For example, the Zika virus NS3 protein was reported to interact with the 14-3-3 protein to evade innate immunity (Riedl et al., 2019), and the Nipah virus W protein hijacks 14-3-3 proteins to inhibit the proinflamatory response (Enchery et al., 2021); this phenomenon has also been described for the Hendra virus W protein (Edwards et al., 2020). Superposition of the SARS-CoV-2N peptide bound to 14-3-3 with from Nipah virus W protein (PDB ID:6W0L (Edwards et al., 2020)) (Fig. 2A) and bound to the E6 protein of HPV type 18 (PDB ID 6ZFD, (Gogl et al., 2021)) (Fig. 2B) reveals significant differences except for the very conserved central phosphoserine and the arginine residue in the −2 position.

It is not yet clear why SARS-CoV-2 harnesses 14-3-3 proteins. In the case of SARS-CoV, it was proposed that 14-3-3 proteins mediate the translocation of the phosphorylated N protein to cytoplasm (Surjit et al., 2005). For SARS-CoV-2, it was proposed that sequestration by 14-3-3 proteins is a cellular response mechanism to inhibit the virus (Tung and Limtung, 2020). Nevertheless, crystal structures are a necessary prerequisite for structure-based inhibitor design (Mejdrova et al., 2017; Otava et al., 2021; Rosas-Lemus et al., 2020). The structure of the SARS-CoV-2N phosphopeptide bound to 14-3-3 could service inhibitor design, albeit it remains to be seen if the SARS-CoV-2 N protein interaction with 14-3-3 is a viable druggable target.

Declaration of Competing Interest

The authors declare that they have no known competing financial interests or personal relationships that could have appeared to influence the work reported in this paper.

Acknowledgments

We are grateful to Miroslava Blechová for the chemical synthesis of the phosphorylated N peptide (194-SRNpSTPG-200). The project was supported by the European Regional Development Fund; OP RDE; Project: "Chemical biology for drugging undruggable targets (Chem-BioDrug)" (No. CZ.02.1.01/0.0/0.0/16_019/0000729). The Academy of Sciences of the Czech Republic (RVO: 61388963) is also acknowledged.

Appendix A. Supplementary material

Supplementary data to this article can be found online at https://doi.org/10.1016/j.jsb.2022.107879.

References

Afonine, P.V., Poon, B.K., Read, R.J., Sobolev, O.V., Terwilliger, T.C., Urzhumtsev, A., Adams, P.D., 2018. Real-space refinement in PHENIX for cryo-EM and crystallography. Acta Crystallogr. D 74 (6), 531–544.

Alblova, M., Smidova, A., Docekal, V., Vesely, J., Herman, P., Obsilova, V., Obsil, T., 2017. Molecular basis of the 14-3-3 protein-dependent activation of yeast neutral trehalase Nth1. In: Proceedings of the National Academy of Sciences of the United States of America 114, E9811–E9820.

Bai, Z., Cao, Y., Liu, W., Li, J., 2021. The SARS-CoV-2 nucleocapsid protein and its role in viral structure, biological functions, and a potential target for drug or vaccine mitigation. Viruses 13 (6), 1115. https://doi.org/10.3390/v13061115.

Boon, S.S., Banks, L., 2013. High-risk human papillomavirus E6 oncoproteins interact with 14-3-3 zeta in a PDZ binding motif-dependent manner. J. Virol. 87, 1586–1595.

Carlson, C.R., Asfaha, J.B., Ghent, C.M., Howard, C.J., Hartooni, N., Safari, M., Frankel, A.D., Morgan, D.O., 2020. Phosphoregulation of phase separation by the SARS-CoV-2 N protein suggests a biophysical basis for its dual functions. Mol. Cell 80, 1092.

Chalupska, D., Eisenreichova, A., Rozycki, B., Rezabkova, L., Humpolickova, J., Klima, M., Boura, E., 2017. Structural analysis of phosphatidylinositol 4-kinase IIIbeta (PI4KB) – 14-3-3 protein complex reveals internal flexibility and explains 14-3-3 mediated protection from degradation in vitro. J. Struct. Biol. 200, 36–44.

Edwards, M.R., Hoad, M., Tsimbalyuk, S., Menicucci, A.R., Messaoudi, I., Forwood, J.K., Basler, C.F., 2020. Henipavirus W proteins interact with 14-3-3 to modulate host gene expression. J. Virol. 94.

Eisenreichova, A., Klima, M., Boura, E., 2016. Crystal structures of a yeast 14-3-3 protein from Lachancea thermotolerans in the unliganded form and bound to a human lipid kinase PI4KB-derived peptide reveal high evolutionary conservation. Acta Crystallogr. F. Struct. Biol. Commun. 72, 799–803.

Enchery, F., Dumont, C., Iampietro, M., Pelissier, R., Aurine, N., Bloyet, L.M., Carbonnelle, C., Mathieu, C., Journo, C., Gerlier, D., Horvat, B., 2021. Nipah virus W protein harnesses nuclear 14-3-3 to inhibit NF-kappa B-induced proinflammatory response. Commun. Biol. 4.

Gao, T.Y., Gao, Y.D., Liu, X.X., Nie, Z.L., Sun, H.L., Lin, K., Peng, H.X., Wang, S.K., 2021. Identification and functional analysis of the SARS-COV-2 nucleocapsid protein. BMC Microbiol. 21.

Gogl, G., Tugaeva, K.V., Eberling, P., Kostmann, C., Trave, G., Sluchanko, N.N., 2021. Hierarchized phosphotarget binding by the seven human 14-3-3 isoforms. Nat. Commun. 12, 1677.

Horvath, M., Petrvalska, O., Herman, P., Obsilova, V., Obsil, T., 2021. 14-3-3 proteins inactivate DAPK2 by promoting its dimerization and protecting key regulatory phosphosites. Commun. Biol. 4.

Liebschner, D., Afonine, P.V., Baker, M.L., Bunkoczi, G., Chen, V.B., Croll, T.I., Hintze, B., Hung, L.W., Jain, S., McCoy, A.J., Moriarty, N.W., Oeffner, R.D., Poon, B.K., Prisant, M.G., Read, R.J., Richardson, J.S., Richardson, D.C., Sammito, M.D., Sobolev, O.V., Stockwell, D.H., Terwilliger, T.C., Urzhumtsev, A.G., Videau, L.L., Williams, C.J., Adams, P.D., 2019. Macromolecular structure determination using X-rays, neutrons and electrons: recent developments in Phenix. Acta Crystallogr. D 75, 861–877.

Mejdrova, I., Chalupska, D., Plackova, P., Muller, C., Sala, M., Klima, M., Baumlova, A., Hrebabecky, H., Prochazkova, E., Dejmek, M., Strunin, D., Weber, J., Lee, G., Matousova, M., Mertlikova-Kaiserova, H., Ziebuhr, J., Birkus, G., Boura, E., Nencka, R., 2017. Rational design of novel highly potent and selective phosphatidylinositol 4-kinase iiibeta (PI4KB) inhibitors as broad-spectrum antiviral agents and tools for chemical biology. J. Med. Chem. 60, 100–118.

Nathan, K.G., Lal, S.K., 2020. The multifarious role of 14-3-3 family of proteins in viral replication. Viruses-Basel 12.

Obsilova, V., Obsil, T., 2020. The 14-3-3 proteins as important allosteric regulators of protein kinases. Int. J. Mol. Sci. 21.

Obsilova, V., Silhan, J., Boura, E., Teisinger, J., Obsil, T., 2008. 14-3-3 proteins: a family of versatile molecular regulators. Physiol. Res./Acad. Sci. Bohemoslov. 57 (Suppl 3), S11–21.

Obsilova, V., Vecer, J., Herman, P., Pabianova, A., Sulc, M., Teisinger, J., Boura, E., Obsil, T., 2005. 14-3-3 Protein interacts with nuclear localization sequence of forkhead transcription factor FoxO4. Biochemistry 44, 11608–11617.

Otava, T., Sala, M., Li, F., Fanfrlik, J., Devkota, K., Perveen, S., Chau, I., Pakarian, P., Hobza, P., Vedadi, M., Boura, E., Nencka, R., 2021. The structure-based design of SARS-CoV-2 nsp14 methyltransferase ligands yields nanomolar inhibitors. ACS Infect. Dis. 7, 2214–2220.

Rezabkova, L., Boura, E., Herman, P., Vecer, J., Bourova, L., Sulc, M., Svoboda, P., Obsilova, V., Obsil, T., 2010. 14-3-3 protein interacts with and affects the structure of RGS domain of regulator of G protein signaling 3 (RGS3). J. Struct. Biol. 170, 451–461.

Riedl, W., Acharya, D., Lee, J.H., Liu, G.Q., Serman, T., Chiang, C., Chan, Y.K., Diamond, M.S., Gack, M.U., 2019. Zika virus NS3 mimics a Cellular 14-3-3-binding motif to antagonize RIG-I- and MDA5-mediated innate immunity. Cell Host Microbe. 26, 493.

Rosas-Lemus, M., Minasov, G., Shuvalova, L., Inniss, N.L., Kiryukhina, O., Brunzelle, J., Satchell, K.J.F., 2020. High-resolution structures of the SARS-CoV-2 2'-O-methyltransferase reveal strategies for structure-based inhibitor design. Sci. Signal. 13.

Rozycki, B., Boura, E., 2022. Conformational ensemble of the full-length SARS-CoV-2 nucleocapsid (N) protein based on molecular simulations and SAXS data. Biophys. Chem. 288, 106843.

Sluchanko, N.N., 2020. Reading the phosphorylation code: binding of the 14-3-3 protein to multivalent client phosphoproteins. Biochem. J 477, 1219–1225.

Surjit, M., Kumar, R., Mishra, R.N., Reddy, M.K., Chow, V.T.K., Lal, S.K., 2005. The severe acute respiratory syndrome coronavirus nucleocapsid protein is phosphorylated and localizes in the cytoplasm by 14-3-3-mediated translocation. J. Virol. 79, 11476–11486.

Tugaeva, K.V., Hawkins, D., Smith, J.L.R., Bayfield, O.W., Ker, D.S., Sysoev, A.A., Klychnikov, O.I., Antson, A.A., Sluchanko, N.N., 2021. The mechanism of SARS-CoV-2 nucleocapsid protein recognition by the human 14-3-3 proteins. J. Mol. Biol. 433, 166875.

Tung, H.Y.L., Limtung, P., 2020. Mutations in the phosphorylation sites of SARS-CoV-2 encoded nucleocapsid protein and structure model of sequestration by protein 14-3-3. Biochem. Biophys. Res. Commun. 532, 134–138.